Temperature Dependent Rate Coefficient for the Reaction $O(^3P) + NO_2 \rightarrow NO + O_2$

Tomasz Gierczak,[†] James B. Burkholder, and A. R. Ravishankara*[,‡]

National Oceanic and Atmospheric Administration, Aeronomy Laboratory, 325 Broadway, Boulder, Colorado 80303, and Cooperative Institute for Research in Environmental Sciences, University of Colorado, Boulder, Colorado 80309

Received: October 5, 1998; In Final Form: December 8, 1998

The rate coefficient (k_1) for the reaction $O(^3P) + NO_2 \rightarrow O_2 + NO$ was measured under pseudo-first-order conditions in $O(^3P)$ atom concentration over the temperature range 220−412 K. Measurements were made using pulsed laser photolysis of NO_2 to produce oxygen atoms and time-resolved vacuum UV resonance fluorescence detection of O atoms. The NO_2 concentration was measured using three techniques: flow rate, UV absorption, and chemical titration ($NO + O_3 \rightarrow NO_2 + O_2$). The NO_2 UV absorption cross section at 413.4 nm was determined as a function of temperature using the chemical titration and flow methods. Including the low-temperature data of Harder et al.[1], the temperature-dependent NO_2 cross section is given by $\sigma_{413.4}(T) = (9.49 - 0.00549\,T) \times 10^{-19}$ cm^2 molecule^{-1}. The measured rate coefficients for reaction 1 can be expressed as $k_1(T) = (5.26 \pm 0.60) \times 10^{-12} \exp[(209 \pm 35)/T]$ cm^3 molecule^{-1} s^{-1}, where the quoted uncertainties are 2σ and include estimated systematic errors. This result is compared with previously reported measurements of k_1.

Introduction

Nitrogen oxides, NO and NO_2 (collectively called NO_x), play a crucial role in atmospheric ozone chemistry: they lead to photochemical ozone production in the troposphere and catalytic ozone destruction in the stratosphere. In the stratosphere, NO_x chemistry affects both the ozone abundance and its vertical profile. Of the many possible catalytic ozone destruction cycles involving NOx, the following is the most important:

$$O(^3P) + NO_2 \rightarrow O_2 + NO \quad (1)$$

$$O_3 + NO \rightarrow O_2 + NO_2 \quad (2)$$

net:

$$O(^3P) + O_3 \rightarrow 2O_2 \quad (3)$$

Atmospheric model calculations of ozone abundances and vertical profiles rely on the temperature-dependent rate coefficients for reactions 1 and 2. Reaction 1 is the rate-limiting step in this catalytic cycle and has been studied many times over the past few decades. However, a careful examination of the available data shows that there are significant discrepancies and that a more accurate rate coefficient would be beneficial.

Current recommendations[2,3] for reaction 1 give $k_1(T) = 6.5 \times 10^{-12} \exp(120/T)$ cm^3 molecule^{-1} s^{-1} and are based on the studies of Davis et al.,[4] Slanger et al.,[5] Bemand et al.,[6] Ongstad and Birks,[7] and Geers-Muller and Stuhl.[8] Other earlier studies, which yielded lower values of k_1(298 K) and positive activation energies, have not been included in deriving the recommendations. The values of k_1(298 K) reported in the above five studies agree within 10%. However, the temperature dependence of k_1 from these studies disagree significantly; the activation energies reported from various groups fall in the range 0 to ∼−400 cal mol^{-1}. The recommended value of the activation energy, 240 ± 240 cal mol^{-1}, has been derived from the studies of Davis et al., Ongstad and Birks, and Geers-Muller and Stuhl. The current recommendations suggest an uncertainty of ∼60% in the value of k_1(200 K); this large range for k_1(200 K) is mostly due to the uncertainty in the activation energy. This level of uncertainty has significant implications in the interpretation of atmospheric measurements of trace species and model calculated abundances and trends of ozone. The rate coefficient has been identified as a major source of uncertainty in stratospheric models (see, for example, ref 9)

Here, we report the temperature dependence of k_1 measured using the technique of pulsed laser photolysis with resonance fluorescence detection of $O(^3P)$ atoms (PP−RF). During these experiments, special emphasis was placed on the determination of NO_2 concentration and measurements of k_1 at stratospheric temperatures. Our results are compared with previous measurements and a new value for stratospheric modeling is suggested.

Experimental Section

The accuracy of the value of k_1, determined in a system where the temporal profile of $O(^3P)$ atoms are measured under pseudo-first-order conditions, depends on how well the concentration of NO_2 is known. Even though NO_2 is a stable gas, there are a few difficulties associated with its handling and knowing its concentration accurately. First, NO_2 can react on the walls of the reactor, thermally decompose (e.g., in electronic flow meters), and be photolyzed by room light. Second, it can undergo self-association

$$2NO_2 \rightleftarrows N_2O_4 \quad (4)$$

[†] Permanent address: Department of Chemistry, Warsaw University, ul. Zwirki i Wigury 101, 02-089 Warszawa, Poland.

* Address correspondence to this author at NOAA/ERL, R/E/AL2, 325 Broadway, Boulder, CO 80303. E-mail: ravi@al.noaa.gov.

[‡] Also affiliated with the Department of Chemistry and Biochemistry, University of Colorado, Boulder, CO 80309.

10.1021/jp983962p CCC: $18.00
Published on Web 02/03/1999

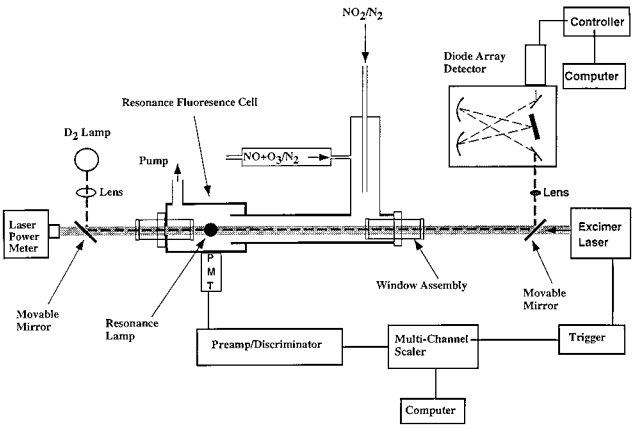

Figure 1. Experimental apparatus used to measure the rate coefficient for reaction 1, $O(^3P) + NO_2 \rightarrow NO + O_2$, utilizing atomic resonance fluorescence detection of O atoms. O atoms were produced by photolysis of NO_2 via an excimer laser. The NO_2 concentration in the reaction cell was determined by UV absorption, flow rate measurements, or chemical titration ($NO + O_3 \rightarrow NO + O_2$) as discussed in the text.

to make significant amounts of N_2O_4 if the NO_2 concentrations are large and/or the temperatures are low ($K_{eq}(T) = 5.2 \times 10^{-29}$ exp(6643/T) cm^3 molecule^{-1} from ref 3). The large temperature dependence of the equilibrium constant can make even small changes in temperature result in significant changes in the NO_2 concentration at low temperatures. This factor alone has limited previous kinetic studies to measurements above 230 K. Third, because k_1 is large, only small concentrations of NO_2 which are difficult to accurately determine, have to be used; otherwise, the loss rate coefficients for $O(^3P)$ atoms exceeds the measurable range ($<10^4$ s^{-1}). In this work, several methods were employed to determine the concentration of NO_2 in the reactor. Use of a combination of these methods reduced the possible systematic errors in NO_2 concentration and, therefore, yielded a more accurate value of k_1. The details of these methods are outlined in a separate section below.

The pulsed photolysis resonance fluorescence (PP−RF) apparatus and the methodology used to measure rate coefficients for $O(^3P)$ atom reactions have been described in detail previously.[10,11] The apparatus was slightly modified for the present study, as shown in Figure 1, to directly measure NO_2 via UV−visible absorption in the reactor. The photolysis laser beam was propagated along the same path as the light beam for absorption measurements. The beams were interchanged by moving two mirrors mounted on repositioning mounts. The metal reaction cell was designed to reduce scattered light and increase the efficiency for detecting fluorescence.[12] A solar blind photomultiplier tube (PMT) detector was mounted orthogonal to both the photolysis laser and resonance lamp to detect the fluorescence. A 1 mm thick CaF_2 window mounted in front of the PMT blocked short wavelength radiation ($\lambda < 130$ nm) from reaching the PMT. The volume between the cell window and the PMT was flushed with N_2 to eliminate absorption of the oxygen atom fluorescence by air. The sensitivity for detection of $O(^3P)$ was nominally $\sim 5 \times 10^8$ atom cm^{-3} for a 1 s integration; this was measured by generating a known concentration of $O(^3P)$ via photolysis of a known concentration of ozone in N_2 at 248 nm using pulsed KrF excimer laser of known fluence. (N_2 quickly quenched $O(^1D)$, formed in ozone photolysis, to $O(^3P)$.)

$O(^3P)$ for measuring k_1 was generated by photolyzing NO_2 at 308 nm (XeCl excimer laser) in the presence of N_2.

$$NO_2 \xrightarrow{h\nu} O(^3P) + NO \quad (5)$$

The yield of $O(^3P)$ in reaction 5 is unity.[3] The $O(^3P)$ atom temporal profile (loss) in the presence of NO_2 was governed by the following processes:

$$O(^3P) + NO_2 \rightarrow O_2 + NO \quad (1)$$

$$O(^3P) + NO \xrightarrow{M} NO_2 \quad (6)$$

$$O(^3P) + \text{impurities} \rightarrow \text{products} \quad (7)$$

$$O(^3P) \rightarrow \text{loss} \quad (8)$$

Reaction 6 needs only to be considered in experiments in which NO was added to the reaction mixture, as described below. Process 7 represents possible loss of $O(^3P)$ via reactions with any impurities in the carrier gas, while reaction 8 represents a pseudo-first-order loss of $O(^3P)$ due to diffusion and flow out of the reaction volume. In our experiments, reactions 7 and 8 were indistinguishable and together accounted for a first-order loss rate constant of ~ 20 s^{-1}. Note that the first-order rate constant for loss of $O(^3P)$ due to reaction 1 was at least five times, and on the average a few hundred times, larger than that due to processes 7 and 8. Oxygen atom temporal profiles were measured under pseudo-first-order conditions, i.e., $[NO_2] \gg [O(^3P)]_o$, with a ratio $[NO_2]/[O(^3P)]_o$ typically $> 2.5 \times 10^3$ (for photolyzing with a 308 nm pulse of ~ 1 mJ cm^{-2}). The exact ratio of $[NO_2]/[O(^3P)]_o$ was controlled by the photolysis laser fluence and was varied over a wide range (~ 0.5 to 7.5 mJ cm^{-2}). The $O(^3P)$ decays were represented by a simple exponential:

$$\ln(S_t) = \ln(S_o) - k't \quad (9)$$

where S_t and S_o are the $O(^3P)$ resonance fluorescence signals at time t and time zero (i.e., right after the photolysis) and

$$k' = k_1[NO_2] + k_6[NO] + k_7[\text{impurity}] + k_8 \quad (10)$$

Approximately 1000−5000 temporal profiles were coadded to improve the signal-to-noise ratio. Measured $O(^3P)$ atom temporal profiles were fit to eq 9 using linear least squares routines to obtain k'. Such temporal profiles were measured at various NO_2 concentrations over the range $(0.04-4) \times 10^{15}$ molecule cm^{-3}. The slope of the plots of k' vs $[NO_2]$ yielded the bimolecular rate coefficient for reaction 1, k_1. The bimolecular rate constants were measured at 15 different temperatures between 220 and 412 K.

All experiments were performed under flow conditions (i.e., flow velocity ≈ 100 cm s^{-1}). The photolysis laser (XeCl excimer laser, 308 nm) beam passed along the length of the absorption cell (parallel to the gas flow). The laser was operated at a repetition rate of 5 Hz. Therefore, the flowing gas sample was exposed to no more than three photolysis laser pulses before reaching the detection zone. At the highest laser fluence, about 0.3% of NO_2 was lost due to photolysis. The kinetic data was not corrected for this small loss.

The temperature of the Pyrex extension (see below) and metal cell, which together formed the absorption cell for measuring the NO_2 concentration, were regulated by flowing either cooled methanol or heated ethylene glycol through their jackets. The temperature was varied over the range 220−412 K. The

temperature of the gas flowing through the cell and the Pyrex extension were measured with a chromel−alumel thermocouple under flow conditions identical to those used in measuring k_1. The temperature was measured at various locations using a retractable thermocouple. The thermocouple was retracted during kinetic measurements. The measured gas temperature was estimated to be accurate to 1 K. A temperature gradient from one end to the other was less than 8 K even at 220 K, the lowest temperature of the experiments. This temperature gradient was sufficiently small as not to affect the NO_2 concentration via N_2O_4 formation or change the effective path length. The temperature in the region where O atoms temporal profiles were measured was constant to better than 0.5 K and was known to better than 0.5 K.

[NO_2] Determination Methods. Three methods were used to determine the NO_2 concentration for measuring k_1: (1) UV absorption, (2) flow, and (3) chemical titration. The UV−vis absorption cross sections of NO_2 were determined using flow, chemical titration, and absolute pressure measurements; hence, using the UV absorption to determine NO_2 concentration was not truly independent of the other two methods. The combination of these methods was used to reduce possible systematic errors associated with the NO_2 concentration determination. Each of these methods is described separately below.

Flow. The rate of change of pressure, dp/dt, in a calibrated volume was measured using a flow of pure NO_2. This flow was added to the measured flows of the other gases, mostly N_2. The pressure in the reactor and the flow tube were measured with 100 Torr electronic capacitance manometers. The concentration of NO_2 was calculated using the measured flow rate of NO_2 and other gases, and pressure in the reactor. The N_2 flow rates were measured using calibrated electronic mass flow meters. This method provided an accurate measurement of NO_2 concentrations for levels below those measurable accurately using UV absorption, $<1 \times 10^{14}$ molecule cm^{-3}. This method was most advantageous for low temperature ($T < 230$ K) measurements where low concentrations of NO_2, $<1 \times 10^{14}$ molecule cm^{-3}, were required to avoid interference from N_2O_4 formation, reaction 4. The overall accuracy of this method was controlled by the accuracy in measuring dp/dt, ±3%, N_2 flow rate, ±3%, and pressure, ±1%, as well as the purity of the NO_2 sample, >99.9%. Thus the absolute accuracy of NO_2 concentrations determined from this method is estimated to be ∼5% by assuming the above uncertainties to be uncorrelated.

Chemical Titration. This method was used to produce NO_2 directly upstream of the absorption cell via the reaction

$$O_3 + NO \rightarrow O_2 + NO_2 \qquad (2)$$

where $k_2(298\ \text{K}) = 1.8 \times 10^{-14}$ cm^3 molecule^{-1} s^{-1}.[3] Note that the measured NO_2 concentration is not dependent on the exact value of this rate constant because all O_3 was converted to NO_2. NO was used in excess over O_3, and the reaction was run to completion (i.e., more than five lifetimes with respect to reaction 2) in a sidearm reactor (Pyrex, 3 cm i.d. and 20 cm long). The residence time of the gas in the reactor was about 2 s. The loss of O_3 and formation of NO_2 were monitored simultaneously by UV absorption with the diode array spectrometer. Concentrations of NO were determined by the dp/dt method, which was described above for the case of NO_2. The concentration of NO was in the range (1 to 8) $\times 10^{14}$ molecule cm^{-3}. The initial ozone concentration was calculated using its absorption spectrum measured using the diode array spectrometer and the known absorption cross section at 253.7 nm. In some experiments, the concentration of NO was held constant while varying the concentration of O_3 that was added to change the NO_2 concentration. In most experiments, the concentration of NO was varied along with that of O_3 to ensure that all the ozone reacted and, yet, had the minimum amount of NO left over. At low O_3 concentrations, NO_2 formed upon addition of NO could not be measured by absorption because its absorption cross section is low, approximately a factor of 20 lower than that of ozone. In these cases, total conversion of O_3 to NO_2 was assumed. The concentration of N_2O_3 was calculated, on the basis of the known equilibrium constants,[3] to be always less than 0.6% of the NO_2 concentration. Only for the measurements at 220 K were the corrections for N_2O_4 significant, i.e., 4% at the highest NO_2 concentration used.

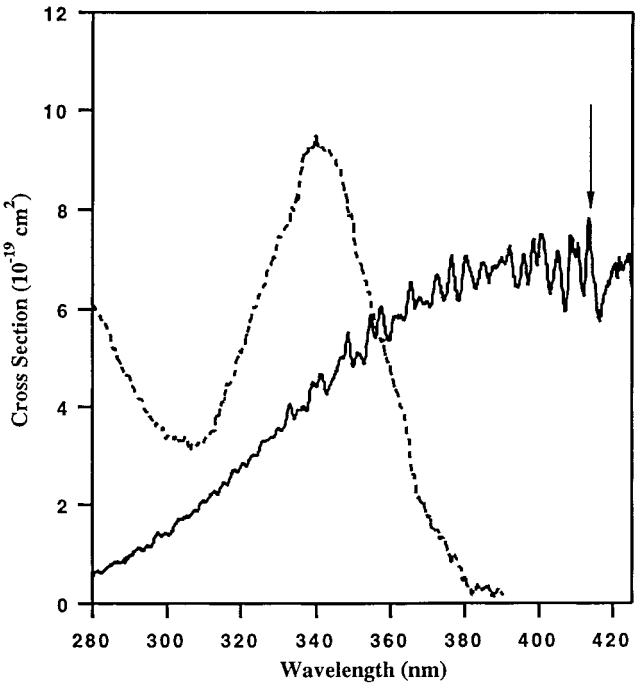

Figure 2. UV absorption spectra of NO_2 (solid line) and N_2O_4 (dashed line) over the range used by the diode array spectrometer. The arrow indicates the location of the NO_2 feature used in the cross section determinations (see text for details).

The accuracy of this [NO_2] determination method is estimated to be ∼5%. This estimate is determined from the uncertainty in the O_3 absorption cross sections, ±2%, and the precision of the absorption measurements, ±3%.

NO_2 UV Absorption. In this method the concentration of NO_2 was measured by UV−visible absorption. The collimated output of a 30 W D_2 lamp was passed through the cell (see Figure 1) and was focused onto the entrance slit of a spectrograph with a 1024 element diode array detector. The combined path through the metal reactor and the Pyrex extension was 42.1 cm. A 100 μm entrance slit, resolution of ∼1 nm, was used for all absorption measurements. The wavelength of the spectrometer was calibrated using a Hg pen ray lamp and a 10 μm entrance slit. The NO_2 spectrum was recorded between 280 and 420 nm. A spectrum of NO_2 in this wavelength region is shown in Figure 2. The prominent absorption feature at 413.4 nm was chosen for NO_2 concentration quantification. At this wavelength, the contribution of N_2O_4, if present, would be minimal (see Figure 2) and the NO_2 cross section is near its maximum value. The NO_2 spectrum contains diffuse structure at this resolution and the cross sections depend on both temperature and resolution.

NO_2 absorption cross sections have been previously measured[3] and recently remeasured in several laboratories[1,13,14] using

spectrometers with different resolutions. Harder et al.[1] have provided high-resolution measurements at 216, 230, 238, and 293 K. Cross sections at lower resolution were calculated from these measurements. However, there is limited cross section data available at temperatures above 298 K. Therefore, we measured NO_2 cross sections over the temperature range 259−385 K using the same spectrograph used in the kinetic measurements, i.e., the same resolution. The measurements of Harder et al. were used to confirm our low-temperature measurement and help establish an empirical relationship between the cross section and temperature.

The NO_2 cross sections were determined using known concentrations of NO_2 generated by the titration reaction 11 as described above. The absorption cross section for NO_2 at 308 nm is $\sim 2 \times 10^{-19}$ cm^2 molecule^{-1} (see Figure 1).

Material. NO_2 was prepared by reacting purified NO with excess O_2 which had been passed through a molecular sieve trap at dry ice temperature. NO_2 was collected in a dry ice cooled trap and purified by trap-to-trap distillation in an excess O_2 flow until a pure white solid remained. The major impurities (<0.1%) in our sample of NO_2 are NO and O_2, whose reactions with O atoms are slow compared to reaction 1. Because k_1 is so large, impurities do not contribute significantly to its measured value, unless the impurity levels reach a few percent. NO (C. P. Grade) was purified by passage through the silica gel trap at dry ice temperature. N_2 (UHP, 99.9995%) was used as the carrier gas in all experiments and was used as supplied.

Results and Discussion

NO_2 Cross-Section Measurements. UV−visible absorption cross sections of NO_2 were determined at five temperatures: 385, 348, 323, 298, and 259 K. Absorbances at 4−6 different NO_2 concentrations were measured at each temperature. Beer's law was obeyed at all temperatures. The cross-section values at 413.4 nm, in units of 10^{-19} cm^2, determined are 7.39 ± 0.07 (385 K), 7.53 ± 0.04 (348 K), 7.72 ± 0.04 (323 K), 7.90 ± 0.06 (298 K), and 7.79 ± 0.11 (259 K). The quoted errors are two standard deviations of the slopes of the absorbance vs concentration plots as determined by linear least-squares analyses. The absolute uncertainty in the cross-section values is estimated to be 3% from the measurements in which both O_3 and NO_2 were measured simultaneously. Our room temperature cross section at 413.4 nm is ∼2% lower than that obtained from Harder et al.[1] and ∼4% lower than that reported by Vandaele et al.[14] The cross sections measured here and those of Harder et al. at 413.4 nm are shown in Figure 3. The agreement between the two sets of measurements is exceptionally good. Our NO_2 cross sections are tied to the cross sections of ozone, which is known to very high accuracy (within 2%)[3]. Thus, normalizing other NO_2 spectra to our cross sections, after properly accounting for differences in resolution, would be reasonable. For a critical evaluation of previous NO_2 cross-section determinations readers are referred to Harder et al.[1]

A weighted linear least-squares fit to the cross sections at 413.4 nm measured by Harder et al. and us yields

$$\sigma_{413.4}(T) = (9.49 - 0.00549T) \times 10^{-19}\,\mathrm{cm}^2 \qquad (11)$$

This relationship was used to calculate the NO_2 cross sections at the temperatures used in the kinetic measurements. The cross section at 413.4 nm was also used to normalize the diode array spectra. On the basis of our measurements and comparison with previous reports, we believe that the absorption cross section of NO_2 at 413.4 nm is known to better than 5% and, hence, our measured concentration of NO_2 in the reactor could have no more than a 5% uncertainty due to its cross section.

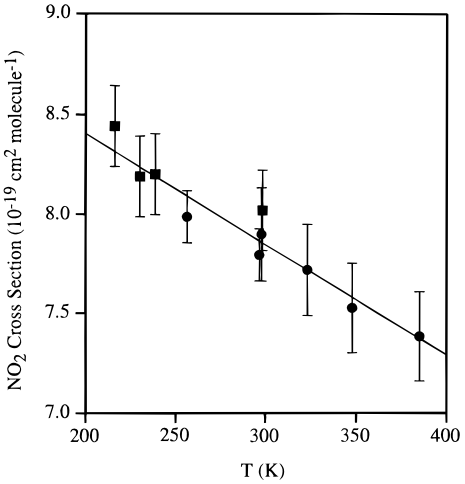

Figure 3. NO_2 UV absorption cross section at 413.4 nm as a function of temperature as determined using methods described in the text. This work (solid circles). Harder et al.[1] (solid squares, after resolution correction). The solid line is the weighted (according to the precision of the measured values) least-squares fit to all the data yielding $\sigma_{413.4}(T) = (9.49-0.00549T) \times 10^{-19}$ cm^2 molecule^{-1}.

Kinetic Measurements. Rate coefficients for reaction 1 were measured at 15 temperatures over the range 220 to 412 K. The results of these measurements are listed in Table 1 and are plotted in Figure 4. A least-squares fit of the data (ln k_1 vs $1/T$) yielded $k_1(T) = (5.26 \pm 0.27) \times 10^{-12} \exp[(209 \pm 15)/T]$ cm^3 molecule^{-1} s^{-1}, where the quoted errors represent 2σ precision of the fit and $\sigma_A = A\sigma_{\ln A}$. The 298 K rate coefficient derived from this fit is 10.6×10^{-12} cm^3 molecule^{-1} s^{-1}, and it agrees with that measured at this temperature; therefore, we quote our 298 K value to be $k_1(298\ \mathrm{K}) = (10.6 \pm 0.8) \times 10^{-12}$ cm^3 molecule^{-1} s^{-1} (Table 2).

Several experimental checks were conducted to ensure that the measured rate coefficients did not depend systematically on the experimental conditions. In three room temperature experiments, the initial (photolytically produced) oxygen atom concentration was varied by a factor of 20. The rate coefficients determined in these measurements agreed to within 8%, well within the estimated accuracy of our measurements.

The pressure was varied between 15 and 105 Torr in two room temperature experiments. This tested for possible interference from the third body reaction

$$O(^3P) + NO_2 \xrightarrow{M} NO_3 \qquad (12)$$

where k_{12}(15 Torr, 298 K) $\sim 4 \times 10^{-14}$ cm^3 molecule^{-1} s^{-1} and k_{12}(105 Torr, 298 K) $= 2.7 \times 10^{-13}$ cm^3 molecule^{-1} s^{-1}.[3] Higher pressures were used only at 298 K and above to test for secondary reactions. Under the low-pressure conditions used here (∼15 Torr), reaction 12 makes a negligible contribution (<1%) to the O(^{3}P) decay even at 220 K, where k_{12}(15 Torr, 220 K) $\sim 1 \times 10^{-13}$ cm^3 molecule^{-1} s^{-1}. Our measured values of k_1 at 15 and 105 Torr total pressure at 298 K agree within the measurement uncertainties (see Table 1). A single elevated pressure measurement, 103 Torr, was also performed at 393 K. The value of k_1 determined under these conditions agreed very well with the value calculated from our Arrhenius fit. These results confirm that reaction 13 was not significant under our conditions.

The methods used for the determination of NO_2 concentration are given in Table 1. In most experiments where the chemical

TABLE 1: Experimental Conditions and Measured Rate Coefficients for $O(^3P) + NO_2 \rightarrow NO + O_2$ (k_1)

T (K)	$[NO_2]$ method[a]	$[O] \times 10^{-11}$ atom cm^{-3}	$[NO_2] \times 10^{-14}$ molecule cm^{-3}	P (Torr)	$k \times 10^{12}$ cm^3 molecule^{-1} s^{-1}
412	O_3 + NO	0.4−2.9	0.15−1.0	15	9.09 ± 0.2
393	abs	1.3−12.7	3.9−37.7	103	9.24 ± 0.3
383	abs	4.4−37.2	2.0−16.7	15	8.57 ± 0.15
364	O_3 + NO	0.3−3.5	0.1−1.2	15	8.96 ± 0.2
348	abs	4.5−35.9	2.0−16.2	15	9.39 ± 0.12
325	O_3 + NO	0.2−1.8	0.08−0.6	15	9.60 ± 0.32
311	abs	0.8−12.5	2.4−36.9	15	10.8 ± 0.5
297	O_3 + NO	10−32.2	4.6 − 12.3	101	10.3 ± 0.2
296	abs	0.4−3.7	3.1−32.6	15	11.0 ± 0.2
296	abs	1.7−28.7	1.9−32.5	105	11.0 ± 0.3
296	abs	7.6−74.3	4.0−39.2	15	10.2 ± 0.3
296	dp/dt	0.4−4.6	0.1−1.1	15	10.5 ± 0.5
298		average			10.7 ± 0.8[b]
271	O_3 + NO/abs	1.9−18.9	2.2−21.7	15	11.6 ± 0.2
256.5	abs	1.0−7.6	4.4−33.9	15	12.6 ± 0.2
247	O_3 + NO	0.6−2.2	0.2−0.8	15	12.4 ± 0.8
236.5	O_3 + NO	0.3−3.0	0.1−1.0	15	12.6 ± 0.3
234	O_3 + NO	0.2−2.1	0.06−0.8	15	12.7 ± 0.5
227	dp/dt	0.6−2.2	0.2−0.8	15	12.4 ± 0.05
220	O_3 + NO	0.1−2.0	0.04−0.6	15	13.7 ± 0.52

[a] O_3 + NO indicates that the NO_2 concentration was measured by converting a measured amount of ozone to NO_2 via reaction with NO. abs indicates that NO_2 was measured via UV absorption at 413.4 nm. dp/dt indicates the NO_2 concentration was measured by determining the time rate of change of pressure in a known volume as NO_2 was flowed into it. (See text for details.) [b] The value was obtained by correcting the values measured close to 298 K for the difference in temperature using the E/R measured here and averaging them. The quoted uncertainty is 2σ of the average.

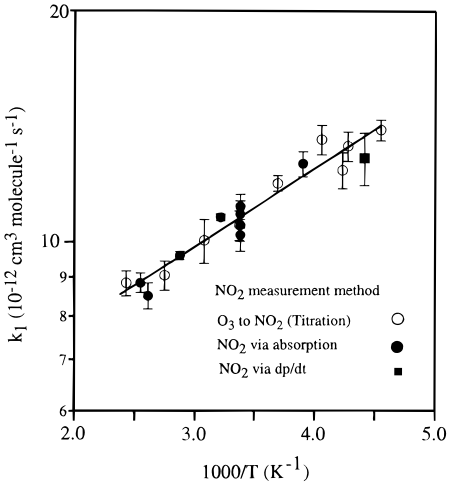

Figure 4. The temperature dependence of the rate coefficient for $O(^3P) + NO_2 \rightarrow NO + O_2$ (k_1) measured in this work. The solid line is the weighted (according to the precision of the measured rate constants) least-squares fit.

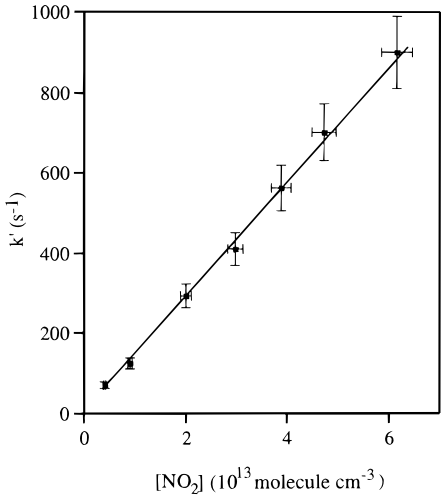

Figure 5. Plot of k' verses $[NO_2]$ at 220 K. The NO_2 concentration has been corrected for the formation of N_2O_4 and contributions to the O atom loss due to the O + NO reaction. The solid line is a weighted (according to the precision of the measured k') least-squares fit to the data yielding a rate coefficient for reaction 1 of 13.7×10^{-12} cm^3 molecule^{-1} s^{-1}.

titration method was used, the NO concentration was only in slight excess to limit contributions to the $O(^3P)$ atom decay from the reaction

$$O(^3P) + NO \xrightarrow{M} NO_2 \qquad (6)$$

where $k_6 \sim 4 \times 10^{-14}$ at 298 K and 15 Torr.[3] The measured pseudo-first-order rates were corrected for reaction 6 using the measured NO concentration. The corrections ranged from 50 to 130 s^{-1}, which are small (less than 3%) compared to the first-order loss rate constants due to reaction 1. When a constant concentration of NO was used, the contribution to measured k' was an intercept in the k' vs $[NO_2]$ concentration plots.

Geers-Muller and Stuhl[8] have estimated upper limits for the rate coefficients for the reactions

$$O + N_2O_4 \rightarrow \text{products} \qquad (13)$$

and

$$O + N_2O_3 \rightarrow \text{products} \qquad (14)$$

at 199 K to be $k_{13} < 2 \times 10^{-12}$ cm^3 molecule^{-1} s^{-1} and $k_{14} < 4.5 \times 10^{-13}$ cm^3 molecule^{-1} s^{-1}, respectively. Hence, the contributions to the measured O atoms decay rate constants of reactions 13 and 14 are at least 7 and 30 times smaller than the contribution from reaction 1 at 199 K. At warmer temperatures, they are negligibly small. Therefore, reaction 13 and 14 should not significantly influence the measurement of k_1. However, in experiments at temperatures below 230 K where the NO_2 concentration was deduced from flows and chemical titration rather than measured by UV absorption, we corrected the NO_2 concentration for the formation of N_2O_4. Figure 5 shows a plot of k' vs $[NO_2]$ at 220 K, where the deduced $[NO_2]$ was corrected

TABLE 2: Summary of Rate Coefficient Measurements for $O(^3P) + NO_2 \rightarrow NO + O_2$ (k_1)

k(298 K)[a]	A[a]	$-E/R$ (K)	T Range (K)	experimental technique[b]	ref
9.12 ± 0.46	8.70 ± 0.65	13 ± 21	230−339	FP−RF	4
9.5 ± 1.1	3.72 ± 0.30	267 ± 30	298−1055	DF−RF/MS	6
9.3 ± 1.4[c]	5.53	154	240−296	FP−CL	5
10.3 ± 0.9	6.58 ± 0.52	142 ± 23	224−354	DF−CL	7
10.3 ± 0.2[d]	5.21 ± 0.50	202 ± 27	233−357	FP−CL	8
9.7[e]	6.5	120 ± 120			2,3
10.6 ± 0.8	5.26 ± 0.6	209 ± 35	220−412	PP−RF	this work
10.6[e]	5.22	210 ± 30			rec.[f]

[a] Units are 10^{-12} cm^3 molecule^{-1} s^{-1}. [b] FP: flash photolysis. DF: discharge flow. RF: resonance fluorescence. MS: mass spectrometry. CL: chemical luminescence. PP: pulse photolysis. [c] k(296 K). [d] Calculated from value measured at 301 K using $E/R = -202$ K^{-1}. [e] Uncertainty of $f(298) = 1.1$. Uncertainties at other temperatures are calculated using $f(T) = f(298)\exp|\Delta E/R\{(1/T) - (1/298)\}|$. [f] Recommended based on results of this study and refs 7 and 8.

for the formation of N_2O_4 using the equilibrium constant.[3] These corrections were small and amounted to a change in rate constant of ~7%. Therefore, even if the equilibrium constant were somewhat uncertain, the rate coefficients would not change much.

The fits of k' vs [NO_2], and hence the obtained values of k_1, were precise. However, this is not a true representation of the reproducibility between measurements. The expression for k_1 given above does include, to a first approximation, the systematic errors in the NO_2 concentration measurements because multiple methods were used. Yet, we include other estimated systematic errors, derived for each NO_2 concentration method, and suggest the following expression for k_1 as a function of temperature:

$$k_1(T) = (5.26 \pm 0.60) \times 10^{-12} \times \exp[(209 \pm 35)/T] \text{ cm}^3 \text{ molecule}^{-1} \text{ s}^{-1}$$

There are a number of relatively recent kinetic studies[4−8] of reaction 1 with which to compare and contrast our results. An overview of our results and those from previous works is given in Table 2. The recent report of $k_1(298\text{ K}) = (9.3 \pm 1.0) \times 10^{-12}$ cm^3 molecule^{-1} s^{-1} reported by Paulson et al.[15] is not included in the table. Davis et al.[4] studied reaction 1 using broadband flash photolysis of NO_2 to produce O atoms and vacuum UV resonance fluorescence to detect them. They measured k_1 over the temperature range 230 to 339 K. The range of NO_2 concentrations used was sufficiently low that corrections for N_2O_4 were small even at the lowest temperatures used. They determined the NO_2 concentrations using manometrically prepared gas mixtures in Ar, N_2, O_2, and CO_2 used as the buffer gas. (Their stock mixtures necessarily had much higher concentrations of NO_2 than those present in the reactor.) The details of the mixture preparation methods was not provided (i.e., the corrections for N_2O_4 in the stock mixture are not known and could have led to small overestimation of NO_2 and, hence, the lower values of k_1). They report $k_1 = (9.12 \pm 0.44) \times 10^{-12}$ cm^3 molecule^{-1} s^{-1} independent of temperature. The quoted error limit is 1σ of the measurement precision and does not include possible systematic errors. This value is about 10% smaller than our room temperature value but within the combined 2σ uncertainty limits. The experimental technique used by Davis et al. was similar to that used in our work, but with a few significant differences. In our experiments the gas mixture was flowed through the reactor, a laser was used to photolyze NO_2 at a single wavelength, the mixture was exposed to at most two photolysis pulses, and NO_2 was directly measured in the reactor in most cases. Davis et al. used a static mixture, broadband photolysis, and exposure of the mixture to multiple photolysis pulses, and deduced the concentration of NO_2 using manometrically prepared stock mixtures. Considering these differences the agreement with our results is surprisingly good. Due to the limitations in the precision of their measurements the weak temperature dependence of k_1 eluded their detection. It is very important to note that Davis et al.'s experiments were excellent for that period, and we have learned much since then as to how to handle gases such as NO_2.

Bemand et al.[6] studied reaction 1 under pseudo-first-order conditions using a discharge flow tube and detected O atoms via resonance fluorescence (in an excess of NO_2) and NO_2 via mass spectrometry (in excess of O atoms) to determine k_1 at sixteen temperatures between 298 and 1055 K. In experiments with NO_2 in excess, the NO_2 concentration was varied over the range $(0.4-4) \times 10^{13}$ molecule cm^{-3}. NO_2 concentrations were determined using flow measurements. Under these conditions, N_2O_4 formation was negligible. In experiments with $O(^3P)$ atoms in excess, the $O(^3P)$ atom concentration was varied over the range (4 to 26) $\times 10^{12}$ atom cm^{-3}. The rate coefficient data measured at each temperature shows considerable scatter with values differing by as much as 50%. Fitting the data given in their Table 1 (weighting the 298 K value by a factor of 20, the number of 298 K values measured by them) yields $k_1(T) = (3.68 \pm 1.0) \times 10^{-12} \exp[(274 \pm 80)/T]$ cm^3 molecule^{-1} s^{-1}, $k_1(298) = 9.3 \times 10^{-12}$ cm^3 molecule^{-1} s^{-1}, where the error limits are 1σ precision of the fit. This fit yields values of k_1 which are systematically lower than our measurements, ~6%, over our temperature range. However, these differences are small compared to the accuracy of the measurements reported by Bemand et al. Also, the possibility of thermal decomposition of NO_2 in their system at high temperatures could have led to the higher negative temperature dependence that they reported.

Slanger et al.[5] measured k_1 using pulsed photolysis of O_2 at 147 nm to generate $O(^3P)$ atoms in the presence of excess NO_2. $O(^3P)$ atoms were detected by reacting it with NO and measuring the chemiluminescence from the NO_2 product. NO_2 concentrations in the range $(0.6-6) \times 10^{13}$ molecule cm^{-3} were used. NO_2 concentrations were determined by UV absorption of a NO_2/N_2 mixture prior to being diluted in the reaction gas mixture. Small corrections were applied to account for N_2O_4 formation. Measurements were made at 296 and 240 K yielding k_1 values of $(9.3 \pm 1.4) \times 10^{-12}$ cm^3 molecule^{-1} s^{-1} and $(10.5 \pm 1.6) \times 10^{-12}$ cm^3 molecule^{-1} s^{-1}, respectively. These results indicate a small negative temperature dependence and are systematically less than our results but are within the combined uncertainties of the two data sets.

Ongstad and Birks[7] used a discharge flow tube reactor and also detected O atoms by the chemiluminescence method. They measured k_1 at six temperatures in the range 224 to 354 K at 2.5 Torr total pressure. Their NO_2 concentrations were calculated from measured flow rates of manometrically prepared gas

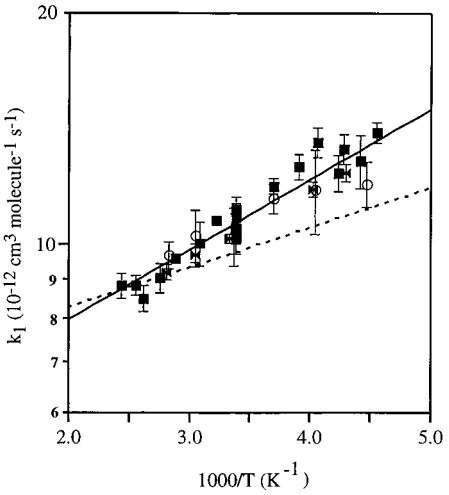

Figure 6. Comparison of recent reaction 1 rate coefficient measurements and current value recommended for stratospheric model calculations (dashed line). The heavy solid line is a weighted least-squares fit to the data from this work (solid squares) and that of Ongstad and Birks[7] (open circles) and Geers-Muller and Stuhl[8] (solid bow tie) yielding a value of $k_1(T) = (5.22 \pm 0.50) \times 10^{-12} \exp[(210 \pm 30)/T]$ cm^3 $molecule^{-1}$ s^{-1}.

mixtures. NO_2 concentrations were varied over the range $(1-10) \times 10^{12}$ molecule cm^{-3}. These low NO_2 concentrations made corrections for N_2O_4 formation negligible at all temperatures. They report $k_1(T) = (6.58 \pm 0.52) \times 10^{-12} \exp[(142 \pm 23)/T]$ cm^3 $molecule^{-1}$ s^{-1}, $k_1(298) = 1.06 \times 10^{-11}$ cm^3 $molecule^{-1}$ s^{-1}, where the error limits are 1σ and represent the precision of the measurements only. Their room temperature value is in excellent agreement with the present results while the temperature dependence, E/R, is smaller but lies within the combined 2σ uncertainty limits.

Geers-Muller and Stuhl[8] used pulsed H_2 laser (~160 nm) photolysis of NO to produce $O(^3P)$ atoms in the presence of NO_2. They measured the temporal profile of $O(^3P)$ using the chemiluminescence method noted above and obtained k_1 at five temperatures over the range 233−357 K using NO_2 concentrations in the range $(0.5-4) \times 10^{14}$ molecule cm^{-3}. NO_2 concentrations were calculated using mass flow rates measured with calibrated flow controllers. Corrections to the NO_2 concentration due to N_2O_4 formation were less than 4% under these conditions. The addition of NO, 8×10^{15} molecule cm^{-3}, in the detection region led to the formation of N_2O_3 via

$$NO + NO_2 + M \leftrightarrow N_2O_3 + M \qquad (15)$$

However, corrections to the NO_2 concentration were less than 1.4% under these conditions. They report $k_1(T) = (5.21 \pm 0.50) \times 10^{-12} \exp[(202 \pm 27)/T]$ cm^3 $molecule^{-1}$ s^{-1}, $k_1(298) = 1.03 \times 10^{-11}$ cm^3 $molecule^{-1}$ s^{-1}, where the quoted error limits are 3σ and include estimated systematic errors. This value is in excellent agreement with our results with k_1 at 233 K only 5% less than the value derived from the present results.

From the above description, it is clear that there are reasons to suspect that the data of Davis et al. may not be highly accurate, especially at low temperatures. The data of Ongstad and Birks and of Geers-Muller and Stuhl are quite accurate. Figure 6 shows a plot of the data obtained by these two groups, along with those from our study. The data from these three studies were fit to the Arrhenius expression using an unweighted linear least squares routine ($\ln k_1$ vs $1/T$) to obtain:

$$k_1(T) = (5.22 \pm 0.50) \times 10^{-12} \times \exp[(210 \pm 26)/T]\ cm^3\ molecule^{-1}\ s^{-1}$$

where the errors are 2σ of the fit and $\sigma_A = A\ \sigma_{\ln A}$. The fit is also shown in the figure. This expression may be used for modeling studies. It should be noted that this lies beyond the 1σ error bounds indicated by 1997-NASA/JPL evaluation. The numbers that can be used for modeling studies are listed in the last row of Table 2.

Atmospheric implications. The rate coefficient obtained in this study is approximately 20−30% higher than that derived in the current kinetic evaluations at stratospheric temperatures.[3] Given that reaction 1 is the rate-limiting step in the major NO_x catalyzed ozone destruction cycle (see Introduction), this change in the rate coefficient will have a significant impact on the calculated stratospheric ozone abundance. Further, increases in k_1 will alter the calculated ozone depletion due to chlorine and the impact of aircraft emissions on ozone levels. We have discussed some these consequences in a separate paper[16] which reexamines the role of NO_x in the stratosphere in light of the changes in the rate coefficients for the reactions of OH with HNO_3 ref 17 and NO_2 (ref 18) as well as k_1.

Acknowledgment. We thank J. Harder for useful discussions and spectroscopic calculations. This work was supported in part by NASA Upper Atmospheric Research Program.

References and Notes

(1) Harder, J. W.; Brault, J. W.; Johnston, P. V.; Mount, G. H. *J. Geophys. Res.* **1997**, *102*, 3861.

(2) Atkinson, R.; Baulch, D. L.; Cox, R. A.; Hampson, R. F.; Kerr, J. A.; Rossi, M. J.; Troe, J. *J. Phys. Chem. Ref. Data* **1997**, *26*, 521.

(3) DeMore, W. B.; Sander, S. P.; Golden, D. M.; Hampson, R. F.; Kurylo, M. J.; Howard, C. J.; Ravishankara, A. R.; Kolb, C. E.; Molina, M. J. Chemical Kinetics and Photochemical Data for Use in Stratospheric Modeling. Evaluation No. 12; Jet Propulsion Laboratory: Pasadena, CA, 1997.

(4) Davis, D. D.; Herron, J. T.; Huie, R. E. *J. Chem. Phys.* **1973**, *58*, 530.

(5) Slanger, T. G.; Wood, B. J.; Black, G. *Int. J. Chem. Kinet.* **1973**, *5*, 615.

(6) Bemand, P. P.; Clyne, M. A. A.; Watson, R. T. *J. Chem. Soc., Faraday Trans. 2* **1974**, *70*, 564.

(7) Ongstad, A. P.; Birks, J. W. *J. Chem. Phys.* **1984**, *81*, 3922.

(8) Geers-Muller, R.; Stuhl, F. *Chem. Phys. Lett.* **1987**, *135*, 263.

(9) Dubey, M. K.; Smith, G. P.; Hartley, W. S.; Kinnison, D. E.; Connell, P. S. *Geophys. Res. Lett.* **1997**, *24*, 2737.

(10) Nicovich, J. M.; Wine, P. H.; Ravishankara, A. R. *J. Chem. Phys.* **1988**, *89*, 5670.

(11) Vaghjiani, G. L.; Ravishankara, A. R. *Int. J. Chem. Kinet.* **1990**, *22*, 351.

(12) Goldfarb, L. The photochemistry and kinetics of chlorine compounds important to stratospheric mid-latitude ozone destruction. Ph.D. Thesis, University of Colorado, 1997.

(13) Harwood: M. H.; Jones, R. L. *J. Geophys. Res.* **1994**, *99*, 22955−22964.

(14) Vandaele, A. C.; Hermans, C.; Simon, P. C.; Carleer, M.; Colin, R.; Fally, S.; Merienne, M. F.; Jenouvrier, A.; Coquart, B. *J. Quant. Spectrosc. Radiat. Transfer* **1998**, *59*, 171.

(15) Paulson, S. E.; Orlando, J. J.; Tyndall, G. S.; Calvert, J. G. *Int. J. Chem. Kinet.* **1995**, *27*, 997.

(16) Brown, S.; Gierczak, T.; Portmann, R. W.; Talukdar, R. K.; Burkholder, J. B.; Ravishankara, A. R. *Geophys. Res. Lett.* Submitted for publication.

(17) Brown, S.; Talukdar, R. K.; Ravishankara, A. R. *J. Phys. Chem.*, 1998. Submitted for publication.

(18) Brown, S.; Talukdar, R. K.; Ravishankara, A. R. *Chem. Phys. Lett.* **1999**, *299*, 217.